Insulating Nature of Strongly Correlated Massless Dirac Fermions in an Organic Crystal

Dong Liu,[1] Kyohei Ishikawa,[1] Ryosuke Takehara,[1] Kazuya Miyagawa,[1]
Masafumi Tamura,[2] and Kazushi Kanoda[1]

[1]*Department of Applied Physics, University of Tokyo, Bunkyo-ku, Tokyo 113-8656, Japan*
[2]*Department of Physics, Faculty of Science and Technology, Tokyo University of Science,
Noda, Chiba 278-8510, Japan*

Through resistivity measurements of an organic crystal hosting massless Dirac fermions with a charge-ordering instability, we reveal the effect of interactions among massless Dirac fermions on the charge transport. A low-temperature resistivity upturn appears robustly irrespective of the pressure and is enhanced while approaching the critical pressure of charge ordering, indicating that the insulating behavior originates from short-range Coulomb interactions. The observation of an apparently vanishing gap in the charge-ordered phase accords with the theoretical prediction of nontopological edge states.

Strongly interacting electrons and massless Dirac fermions (MDFs) are both of keen interest in condensed matter physics. The interplay between the interactions and the massless nature is a prime issue in the physics of MDFs and has been intensively studied for the single layer of carbon atoms, graphene [1,2]. Even before the successful separation of graphene, renormalization-group studies predicted that the Fermi velocity is logarithmically enhanced on approaching the Dirac point due to the unscreened long-range Coulomb repulsion among electrons [3]. Actually, the quantum oscillations in suspended graphene proved the reshaping of the Dirac cone that results from the velocity renormalization [4]. However, how the resistivity of interacting MDFs behaves is under debate. In the absence of interactions, the Dirac point conductance is theoretically given by the universal quantum value of $4e^2/\pi h$ [5] (with some modification in tilted cones [6]), which had been one of experimental targets in the early stage of the research [7]. In the presence of interactions, it was predicted that the quasiparticle scattering rate of interacting MDFs is proportional to the temperature [8], being distinct from the conventional behavior of Fermi liquids, and the Dirac-point conductance in clean graphene is suggested to increase logarithmically on cooling from the order of $4e^2/\pi h$ around room temperature [9]. The experimental results, however, are not in line with the prediction; σ at the Dirac point decreases at low temperatures, in many cases, following power laws of T but with unsettled exponents [10,11]. These behaviors have been discussed in the light of the inhomogeneity or ripples in real graphene samples suspended or attached on substrates [10,12–15], or the broken valley symmetry under top gating on the BN substrate [11]. The environments appear influential in the low-energy charge transport in graphene. It remains to be answered how the Dirac-point conductance is impacted by the correlation effect.

We tackle this problem with another MDF system, a quasi-two-dimensional organic conductor, α-(BEDT-TTF)$_2$I$_3$ [16,17] (abbreviated as α-I$_3$ hereafter), which is composed of conducting layers of (BEDT-TTF)$^{+1/2}$ cations hosting MDFs [as shown in the inset of Fig. 1(a)] and insulating layers of triiodide anions $(I_3)^{-1}$, where BEDT-TTF stands for bisethylene-dithio-tetrathiafulvalene. This is the first material that exhibits a charge-ordered (CO) state and a MDF state right beside each other in the pressure-temperature phase diagram. At ambient pressure, α-I$_3$ undergoes a transition at 135 K from a conducting state to a CO state with the inversion symmetry broken, where the charge is disproportioned between the two A sites in a unit cell as shown in the inset of Fig. 1(a) [18–23]; however, when the CO state is suppressed by pressure, a MDF phase with the nature of strong correlation emerges [24–26]. Compared with graphene, α-I$_3$ is distinctive in the following respects. (i) A layered bulk crystal of α-I$_3$ is free from both the structural deformation inevitable in free suspension and the influences of substrates, and thus the Dirac point could be approached in a super-clean condition. (ii) Owing to a fixed band filling (3/4) in the crystal, the Fermi energy is exactly located at the charge-neutral Dirac point. (iii) The strength of the electron interactions is systematically varied near the CO-MDF phase boundary by pressure. (iv) The Dirac cone in α-I$_3$ is so largely tilted that the k-dependent Fermi velocity varies over approximately a tenfold range [26].

Earlier transport studies of α-I$_3$ revealed that the resistivity shows an anomalous upturn with a logarithmic increase on cooling [27]. As the upturn is suppressed by carrier doping [28], which makes the Fermi level shift from the Dirac point, the low-temperature upturn is characteristic of the Dirac point. In the present work, we have explored the charge transport in α-I$_3$ in a wide pressure range covering the CO and MDF phases with a particular focus
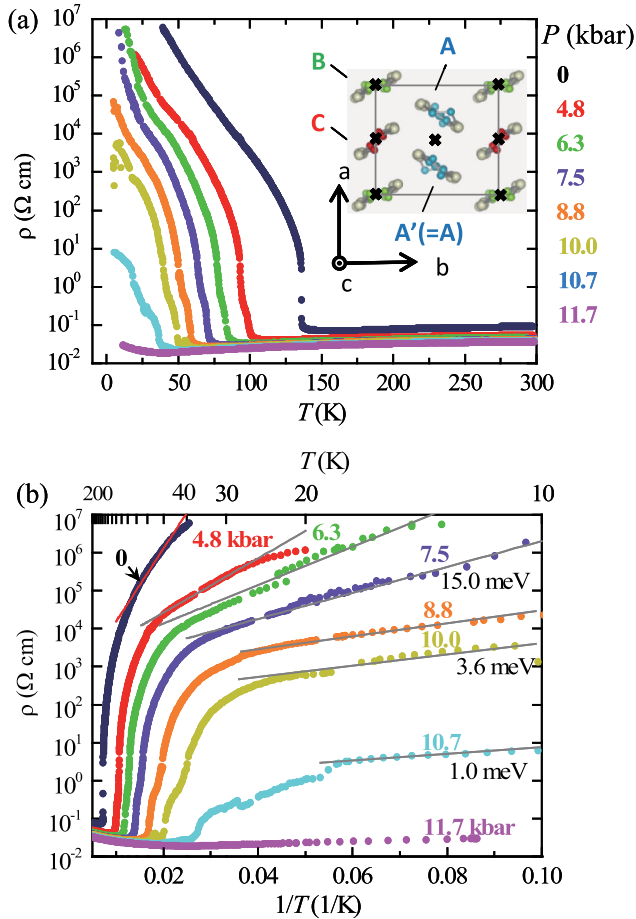
FIG. 1. Temperature dependence of the resistivity (a) and the corresponding Arrhenius plot (b) for α-(BEDT-TTF)$_2$I$_3$ under different pressures. The inset of (a) shows the crystal structure of α-(BEDT-TTF)$_2$I$_3$ viewed from the c axis, namely, the a-b in-plane structure, in the conducting state. The crystallographically inequivalent molecular sites A (A'), B, and C comprise a unit cell as indicated by the square. The black crosses indicate the positions of the inversion centers.

FIG. 2. (a) Pressure-temperature phase diagram. The different symbols indicate the charge-ordering temperatures T_{CO} determined from different crystals. For the definition of T_{CO}, see the text. The solid line is a guide to the eye. T_{min} indicates the temperature at which the resistivity takes a minimum in the massless Dirac fermion state under pressures above 11 kbar. T_{CO} (red circles) and T_{min} are from the same sample. Regions I and II are discussed in the text. (b) Pressure dependence of the activation energy of the Arrhenius plot in Fig. 1(b). The filled and open red circles are from different surface places of the same crystal. The dashed line is a guide to the eye.

on the critical region of the CO-MDF transition to clarify the relationship between the transport anomaly and electron correlations.

Single crystals of α-I$_3$ were synthesized by the conventional electrochemical oxidization method. The typical size of the crystals is 1×0.3 mm in the a-b conducting plane, with a 10 to 100 μm thickness (along the c axis). The in-plane electrical resistivity was measured by the four-terminal method. For applying hydrostatic pressures, we used two clamp-type pressure cells, a BeCu single-wall cell and a BeCu/NiCrAl dual-structured cell, for pressures up to 20 and 40 kbar, respectively. As the pressure-transmitting media, we used Daphne 7373 and 7474 oils, which maintain hydrostaticity up to 20 and 40 kbar, respectively [29]. All the pressure values given below are the values at room temperature before cooling. At ambient pressure, we performed measurements for 13
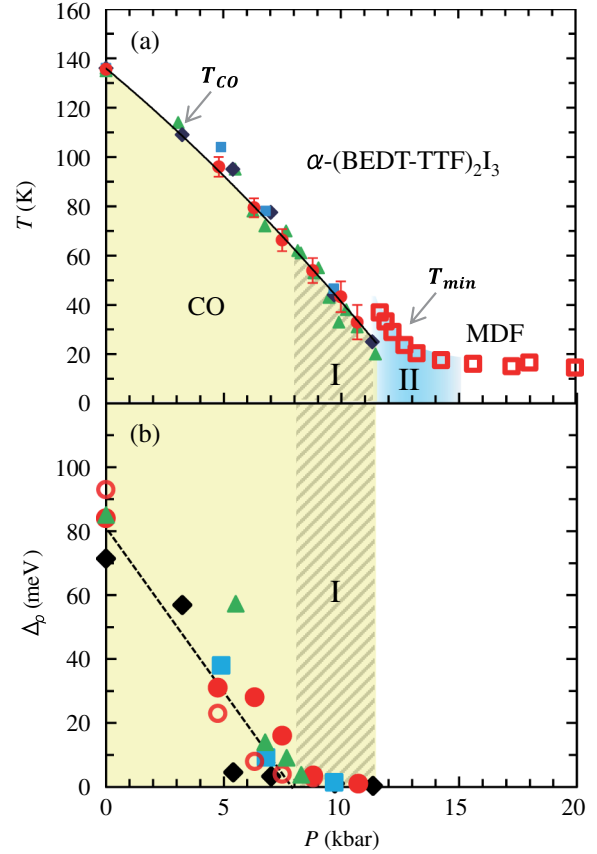
crystals, four of which were further used for experiments up to 13 kbar, and one of the four was measured under increasing pressures up to 20 kbar. We used two separate crystals for higher pressures of 25 to 40 kbar.

Figure 1(a) shows the temperature dependence of the electrical resistivity ρ under increasing pressures for one crystal; the Arrhenius plot of ρ is displayed in Fig. 1(b). The overall characteristic is reproduced by all other crystals. For $P < 11$ kbar, the resistivity shows a steep increase at the CO transition. The transition temperature T_{CO} is determined by a temperature giving a peak in the $-d(\ln \rho)/dT$ versus T^{-1} curve and is shown against pressure in Fig. 2(a) together with the results of all other crystals studied up to 20 kbar. T_{CO} decreases continuously with increasing pressure and eventually vanishes above 11 kbar. Below T_{CO}, the temperature dependence of ρ is not of the ideal Arrhenius type and is somewhat sample
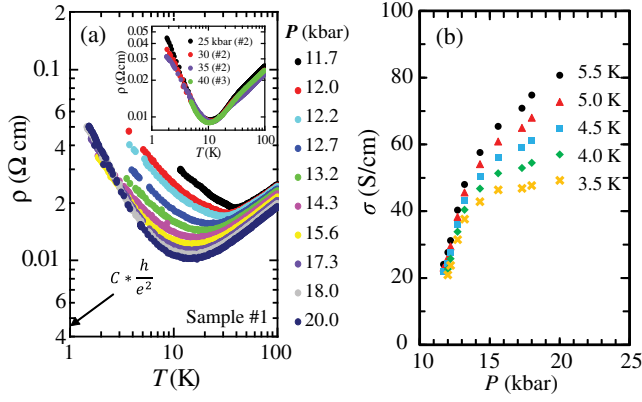
FIG. 3.   (a) Temperature dependence of the resistivity in the massless Dirac fermion state above 11 kbar. Sample 1 covers pressures up to 20 kbar (main panel). Sample 2 was measured at 25, 30, and 35 kbar, and sample 3 was used for the measurements at 40 kbar (inset). The bulk resistivity corresponding to the quantum sheet resistance, $C \times (h/e^2) = 4.5 \times 10^{-3}$ Ωcm, is indicated, where $C = 1.7$ nm is the lattice constant along the c axis [31]] under a pressure of around 20 kbar. (b) Conductivity versus pressure for fixed temperatures above 11 kbar in the low-temperature region, where the resistivity upturn appears.

dependent, as reported earlier (ambient-pressure data) [30]; nevertheless, the activation energies of the Arrhenius plots, Δ_ρ, for all the samples studied exhibit a systematic variation with pressure, as shown in Fig. 2(b). Δ_ρ decreases with increasing pressure more rapidly than T_{CO} does and vanishes around 7–8 kbar. Unexpectedly, the pressure dependence of Δ_ρ does not scale with that of T_{CO} at all and there is a pressure range, as indicated by region I in Fig. 2, where Δ_ρ vanishes while the charge ordering is identified by clear resistive anomalies at T_{CO}. At approximately 11 kbar, T_{CO} drops from 20 to 0 K discontinuously, indicating a CO-MDF phase transition of the first order. These are consistent with the Raman study, which showed that the charge disproportionation ratio 0.2:0.8 between the A and A' sites [Fig. 1(a) inset] at ambient pressure decreases at a rate of ~0.01/kbar with increasing pressure up to 11 kbar and vanishes, at least, at 15 kbar [21].

For pressures above 11 kbar, the resistivity is characterized by metallic but weak temperature dependences followed by anomalous upturns at low temperatures. The high-temperature behavior, which reproduces the previous results [24], is understood in terms of the compensation of the contrasting temperature dependences of the carrier density and the mobility [24]. We particularly focus on the low-temperature upturn observed in the whole pressure range for all the samples measured. At high pressures above 15 kbar, the upturn is nearly pressure insensitive, which is confirmed to persist up to 40 kbar, as shown in Fig. 3(a). It is remarkable that below 15 kbar the low-temperature upturn is enhanced and the enhancement is in a near-critical manner near the CO-MDF transition pressure, indicating the weak first-order nature of the transition at

low temperatures, although ρ at high temperatures is pressure insensitive. Concomitantly, the temperature at which the resistivity takes a minimum, T_{min}, shows an accelerated increase as the pressure is decreased from 15 kbar, as shown in Fig. 2(a). The MDF state is stable and pressure insensitive at high pressures but changes its nature when the CO transition is approached. We denote this transient region as region II in the phase diagram hereafter.

First, we discuss the charge transport in the CO state. At ambient pressure, the Δ_ρ values of the samples studied are in a range of 40 ± 5 meV and thus $2\Delta_\rho$ approximately accords with the optical gap, 75 meV [32]. However, the charge gap under pressure is highly unusual in that Δ_ρ is not scaled to T_{CO} and, in particular, vanishes in region I in spite of the resistivity anomalies signifying the bulk nature of the charge ordering. The contradicting behaviors of T_{CO} and Δ_ρ suggest extraordinarily low-energy charge excitations or the presence of tiny conducting portions or paths in the bulk CO background. In connection with the former possibility, the b axis optical conductivity [32] and dielectric response [33] at ambient pressure exhibit low-energy excitations, which are discussed in terms of phasonlike and domain-wall-like excitations [33]. These excitations, however, are not pertinent to the dc conductivity, as indicated in the present results at ambient pressure and earlier [33]. In the latter case, the coexistence of tiny MDF domains due to the first-order transition or to inhomogeneity in the internal pressure is conceivable. However, it is questionable whether the MDF state stabilized as a bulk phase above 11 kbar appears near ambient pressure even if it is a tiny volume. Alternatively, Omori *et al.* theoretically suggested the appearance of edge states in the CO phase [34]. It is well known that MDF materials are accompanied by peculiar edge or surface states. Zigzag-type edge states in graphene with broken bulk inversion symmetry, acquiring a massive nature, are suggested to vary from a gapped flat band to gapless edge modes with valley polarization by applying a potential on the sample edge [35] or those with valley and spin polarization by turning on edge ferromagnetism [36]. Edge transport is robust against impurities with smooth potentials because of the valley polarization of the gapless edge states [36]. In α-I$_3$, the CO state in the vicinity of the CO-MDF phase boundary was also predicted to be characterized by massive Dirac fermions [37]. The calculations of the edge states in the CO phase upon incorporating the electron correlation found that the energy gap in the edge states formed in between the upper and lower bands in the bulk decreases with the magnitude of the Coulomb interactions, which is varied by the pressure in experiments, and closes before the CO-MDF phase boundary is reached. This can contribute to the transport [34], being fully consistent with the present observation [see Fig. 2(b)]. The predicted edge states are not topologically protected, being distinct from those of topological

insulators [38] and the spin-polarized zero-mode-Landau level of α-I$_3$ [39], and thus are sensitive to the roughness of the edge surfaces. This explains why the absolute value of ρ remains large. A large drop in ρ at 10.7 kbar is likely due to the coexistence of the MDF phase just in the vicinity of the critical pressure.

On entering into the MDF state across the critical pressure of 11 kbar, the charge transport in the MDF state is featured by the characteristic temperature $T_{\min}$ and the magnitude of the associated resistivity upturn at $T < T_{\min}$, both of which are profoundly enhanced near the critical pressure of the CO-MDF transition. The persistence of $T_{\min}$ up to at least 40 kbar indicates that the resistivity upturn at low temperatures is intrinsic to the MDFs but is not due to the inhomogeneous mixture of the CO residues, which only possibly exist just in the vicinity of the critical pressure of the CO-MDF transition. Besides, at the critical pressure P_C, $T_{CO} \sim 20$ K while $T_{\min}$ is ~ 40 K, indicating that the resistivity upturn is not due to the CO residues. The quantum sheet resistance $h/e^2 = 25.8$ kΩ corresponds to the bulk resistivity 4.5×10^{-3} Ω cm, in the present case. The resistivity appears to decrease toward this value before showing an increase [see Fig. 3(a)]. The pressure evolution of the conductivity at $T < T_{\min}$ is such that it decreases and vanishes at 10.5–11 kbar, which is close to the CO-MDF critical pressure, as seen in Fig. 3(b). The pressure dependence of the upturn in region II indicates that the electron correlation is responsible for the upturn because it is enhanced in a quasicritical manner near the correlation-induced transition to the CO state. In the framework of the renormalization of unscreened long-range Coulomb interactions based on the Weyl equation, the conductivity is predicted to increase logarithmically against a temperature decrease [9], in sharp contrast to the experimental features. A disorder-induced localization, a conceivable origin of the resistivity increase, is unlikely to explain the clear pressure dependence of the upturn and the absence of the negative magnetoresistance [28] as observed in graphene [10].

Thus, the present results strongly indicate that the resistivity upturn at low T is due to interactions among MDFs and invoke a notion beyond the conventional framework to treat the interaction effects on MDFs. It is known that in real α-I$_3$ crystals an I$_3^{-1}$ deficiency of several ppm causes the chemical potential to deviate from the Dirac point by the order of a few kelvin, corresponding to submillivolt gating [27]; nevertheless, the upturn was sample independent, indicating that a few kelvin around the Dirac point is a characteristic energy scale where the picture of the renormalized conical dispersion may break down; something unexpected beyond the renormalization may happen in the low energies, the scale of which can be more specifically dictated by a $T_{\min}$ of 10 K. The low-temperature resistivity increase may be an indication of a pseudogap formation in the charge channel, which is enhanced while approaching the MDF-CO phase transition

at $P_C \sim 11$ kbar before forming a real gap in the CO phase. The CO state is stabilized by the intersite Coulomb interactions, which is not incorporated in modeling interacting MDFs in terms of the Weyl equation, which assumes that the MDFs travel in a continuum. In real systems, however, they are on lattices, in which the transfer integrals set the upper limit of the kinetic energy, being exceeded by the short-range interactions in the CO state. The significance of the short-range interactions even in the MDF regime is theoretically argued in terms of the Hubbard model [40]. As the renormalization effect of the long-range Coulomb interactions on the electron velocity is expected to persist without an anomaly at a particular pressure, the short-range part of the Coulomb interactions is likely a key to the anomalous resistivity increase, for example, through charge fluctuations [41] or excitonic fluctuations [42], leading to a possible consequence that the ground state of the interacting MDFs on lattices is insulating.

In conclusion, we investigated the low-temperature resistivity of interacting massless Dirac fermions in an organic crystal, α-(BEDT-TTF)$_2$I$_3$, which is free from the complexities associated with free suspension and attached substrates, around the critical pressure of a transition to the charge-ordered phase. In the massless Dirac fermion phase, increases in the resistivity at low temperatures are confirmed as a robust feature of massless Dirac fermions and found to be enhanced in a near-critical manner while approaching the charge-ordering transition. This is an indication that the resistivity upturn toward an insulating ground state is caused by the interactions of massless Dirac fermions—a novel feature of the interacting Dirac liquid situated in a quantum critical point [43], which shows up when the environmental influences are minimized. In the charge-ordered phase, an apparent suppression of the charge gap with a pressure increase is revealed and found most reasonably explainable in terms of the emergence of the edge states suggested theoretically.

[1] V. N. Kotov, B. Uchoa, V. M. Pereira, F. Guinea, and A. H. Castro Neto, Rev. Mod. Phys. **84**, 1067 (2012).

[2] T. O. Wehling, A. M. Black-Schaffer, and A. V. Balatsky, Adv. Phys. **63**, 1 (2014).

[3] J. Gonzalez, F. Guinea, and M. A. H. Vozmediano, Nucl. Phys. **B424**, 595 (1994).

[4] D. C. Elias, R. V. Gorbachev, A. S. Mayorov, S. V. Morozov, A. A. Zhukov, P. Blake, L. A. Ponomarenko, I. V. Grigorieva, K. S. Novoselov, F. Guinea, and A. K. Geim, Nat. Phys. **7**, 701 (2011).

[5] N. H. Shon and T. Ando, J. Phys. Soc. Jpn. **67**, 2421 (1998).

[6] M. Trescher, B. Sbierski, P. W. Brouwer, and E. J. Bergholtz, Phys. Rev. B **91**, 115135 (2015).

[7] A. K. Geim and K. S. Novoselov, Nat. Mater. **6**, 183 (2007).

[8] J. González, F. Guinea, and M. A. H. Vozmediano, Phys. Rev. Lett. **77**, 3589 (1996).

[9] L. Fritz, J. Schmalian, M. Müller, and S. Sachdev, Phys. Rev. B **78**, 085416 (2008).

[10] L. a. Ponomarenko, a. K. Geim, a. a. Zhukov, R. Jalil, S. V. Morozov, K. S. Novoselov, I. V. Grigorieva, E. H. Hill, V. Cheianov, V. Falko, K. Watanabe, T. Taniguchi, and R. V. Gorbachev, Nat. Phys. **7**, 958 (2011).

[11] F. Amet, J. R. Williams, K. Watanabe, T. Taniguchi, and D. Goldhaber-Gordon, Phys. Rev. Lett. **110**, 216601 (2013).

[12] K. I. Bolotin, K. J. Sikes, J. Hone, H. L. Stormer, and P. Kim, Phys. Rev. Lett. **101**, 096802 (2008).

[13] J. Martin, N. Akerman, G. Ulbricht, T. Lohmann, J. H. Smet, K. Von Klitzing, and A. Yacoby, Nat. Phys. **4**, 144 (2008).

[14] S. Das Sarma, E. H. Hwang, and Q. Li, Phys. Rev. B **85**, 195451 (2012).

[15] I. V. Gornyi, V. Yu. Kachorovskii, and A. D. Mirlin, Phys. Rev. B **86**, 165413 (2012).

[16] K. Bender, K. Dietz, H. Endres, H. W. Helberg, I. Hennig, H. J. Keller, H. W. Schäfer, and D. Schweitzer, Mol. Cryst. Liq. Cryst. **107**, 45 (1984).

[17] K. Bender, I. Hennig, D. Schweitzer, K. Dietz, H. Endres, and H. J. Keller, Mol. Cryst. Liq. Cryst. **108**, 359 (1984).

[18] H. Kino and H. Fukuyama, J. Phys. Soc. Jpn. **64**, 1877 (1995).

[19] H. Seo, J. Phys. Soc. Jpn. **69**, 805 (2000).

[20] Y. Takano, K. Hiraki, H. M. Yamamoto, T. Nakamura, and T. Takahashi, Synth. Met. **120**, 1081 (2001).

[21] R. Wojciechowski, K. Yamamoto, K. Yakushi, M. Inokuchi, and A. Kawamoto, Phys. Rev. B **67**, 224105 (2003).

[22] T. Kakiuchi, Y. Wakabayashi, H. Sawa, T. Takahashi, and T. Nakamura, J. Phys. Soc. Jpn. **76**, 113702 (2007).

[23] K. Yamamoto, S. Iwai, S. Boyko, A. Kashiwazaki, F. Hiramatsu, C. Okabe, N. Nishi, and K. Yakushi, J. Phys. Soc. Jpn. **77**, 074709 (2008).

[24] N. Tajima, M. Tamura, Y. Nishio, K. Kajita, and Y. Iye, J. Phys. Soc. Jpn. **69**, 543 (2000).

[25] H. Kino and T. Miyazaki, J. Phys. Soc. Jpn. **75**, 034704 (2006).

[26] S. Katayama, A. Kobayashi, and Y. Suzumura, J. Phys. Soc. Jpn. **75**, 054705 (2006).

[27] N. Tajima, R. Kato, S. Sugawara, Y. Nishio, and K. Kajita, Phys. Rev. B **85**, 033401 (2012).

[28] K. Kajita, Y. Nishio, N. Tajima, Y. Suzumura, and A. Kobayashi, J. Phys. Soc. Jpn. **83**, 072002 (2014).

[29] K. Murata, K. Yokogawa, H. Yoshino, S. Klotz, P. Munsch, A. Irizawa, M. Nishiyama, K. Iizuka, T. Nanba, T. Okada, Y. Shiraga, and S. Aoyama, Rev. Sci. Instrum. **79**, 085101 (2008).

[30] S. Uji, K. Kodama, K. Sugii, Y. Takahide, T. Terashima, N. Kurita, S. Tsuchiya, M. Kohno, M. Kimata, K. Yamamoto, and K. Yakushi, Phys. Rev. Lett. **110**, 196602 (2013).

[31] R. Kondo, S. Kagoshima, N. Tajima, and R. Kato, J. Phys. Soc. Jpn. **78**, 114714 (2009).

[32] C. Clauss, N. Drichko, D. Schweitzer, and M. Dressel, Physica (Amsterdam) **405B**, S144 (2010).

[33] T. Ivek, B. Korin-Hamzić, O. Milat, S. Tomić, C. Clauss, N. Drichko, D. Schweitzer, and M. Dressel, Phys. Rev. Lett. **104**, 206406 (2010).

[34] Y. Omori, G. Matsuno, and A. Kobayashi, JPS Conf. Proc. **1**, 012119 (2014).

[35] W. Yao, S. A. Yang, and Q. Niu, Phys. Rev. Lett. **102**, 096801 (2009).

[36] Z. Qiao, S. A. Yang, B. Wang, Y. Yao, and Q. Niu, Phys. Rev. B **84**, 035431 (2011).

[37] A. Kobayashi, Y. Suzumura, F. Piéchon, and G. Montambaux, Phys. Rev. B **84**, 075450 (2011).

[38] M. Z. Hasan and C. L. Kane, Rev. Mod. Phys. **82**, 3045 (2010).

[39] T. Osada, J. Phys. Soc. Jpn. **84**, 053704 (2015).

[40] A. Kobayashi and Y. Suzumura, J. Phys. Soc. Jpn. **82**, 054715 (2013).

[41] T. Kanao and M. Ogata (private communication).

[42] G. Matsuno and A. Kobayashi (private communication).

[43] D. E. Sheehy and J. Schmalian, Phys. Rev. Lett. **99**, 226803 (2007).